Journal of Ovarian Research

RESEARCH

Open Access

Ovarian cancer derived extracellular vesicles promote the cancer progression and angiogenesis by mediating M2 macrophages polarization

Xue Tang[1], Chengbin Ma[1], Qiongwei Wu[1] and Meng Yu[1,2*]

Abstract

Background Extracellular vesicles (EVs) are mediators between cancer cells and other types of cells, such as tumor-associated macrophages (TAMs), in the tumor microenvironment. EVs can remodel the tumor microenvironment and regulate tumor progression. However, the underlying molecular mechanism of these interactions remains unclear.

Methods First, we explored the effect of TAMs on the survival prognosis of patients with ovarian cancer. Next, we isolated EVs derived from ovarian cancer cells (OV-EVs) through ultracentrifugation and analyzed the capacity of OV-EVs to regulate macrophage polarization in ovarian tumors and in whole peripheral blood. Moreover, we explored the roles of OV-EVs-induced macrophages in tumor progression through in vitro and in vivo assays.

Results OV-EVs were encapsulated by macrophages and induced the polarization of macrophages toward the M2 phenotype. Moreover, OV-EVs-induced M2 macrophages promoted angiogenesis and cancer progression both in vitro and in vivo. In addition, OV-EVs-induced macrophages increased the expression level of VEGF and increased the expression level of VEGFR in tumors, which resulted in angiogenesis in ovarian cancer.

Conclusions The present study demonstrated that OV-EVs induce M2 polarization in macrophages and promote the progression of ovarian cancer. This study provides novel insight into the mechanism of ovarian cancer progression.

Keywords Extracellular vesicles, Ovarian cancer, Macrophage polarization, Progression, Angiogenesis

Introduction

It is widely acknowledged that ovarian cancer is one of the most common malignant cancers of the female reproductive system [1]. Due to the difficulty in obtaining a diagnosis at an early stage, millions of ovarian cancer patients experience cancer metastasis because of a lack of timely treatment. Despite ongoing efforts in screening programs for ovarian cancer, only a small number of women are diagnosed before the cancer spreads beyond the ovaries [2], and others undergo metastasis throughout the peritoneal cavity, to the omentum [3], and even to the parenchyma of the liver [4] or lung. Thus, a better understanding of the mechanism of ovarian cancer metastasis will provide new insights into ovarian cancer progression and treatments.

*Correspondence:
Meng Yu
fdmdym@126.com
[1] Department of Gynecology, Maternal and Child Healthcare Hospital of Changning District, Shanghai 200135, China
[2] Department of Gynecology, The Obstetrics and Gynecology Hospital of Fudan University, Shanghai, China

Increasing evidence indicates that the process of tumor microenvironment remodeling is closely related to cancer progression. In the tumor microenvironment, the crosstalk between diverse types of cells influences both physiological and pathological processes. Immune cells play vital roles in cancer metastasis and progression. Macrophages are important components of the tumor microenvironment and are associated with cancer progression [5], drug resistance, and immune escape [6], among other effects [7]. Typically, macrophages are divided into M1 and M2 populations [8] to describe the two major and opposing activities of macrophages [9]. M1 macrophages can inhibit cell proliferation and cause tissue damage [10], whereas M2 macrophages can promote cell proliferation and tissue repair [11]. Polarized M2 macrophages can induce premetastatic niche formation and cancer metastasis [12, 13], which are involved in the EMT process [14]. Moreover, some studies have reported that increased VEGF production by lactate-polarized macrophages results in a positive feedback loop that further stimulates angiogenesis [15, 16].

Extracellular vesicles (EVs) are particles derived from diverse types of cells [17] and contain diverse cargos [18, 19]. EVs play vital roles in cell communication and complex interactions during biological processes [20] and pathological processes [21]. It has been widely reported that extracellular vesicles can affect cell proliferation [22], wound healing, systemic metabolism [23], drug resistance and other processes [24, 25]. Additionally, extracellular vesicles mediate the progression of cancers [26, 27], including chemoresistance, metastasis, and immune evasion. However, how ovarian cancer-derived extracellular vesicles interact with macrophages to regulate cancer progression and the underlying molecular mechanisms of diverse types of crosstalk remain unclear.

Vasculogenesis, the formation of blood vessels from de novo generation of endothelial cells, and angiogenesis, the process of new blood vessel formation, are critical during development and subsequent physiological homeostasis but can be pathogenic in cancers. Vascular endothelial-derived growth factor (VEGF), which is important in vasculogenesis and angiogenesis, was identified, isolated, and cloned over two decades ago [28]. VEGF secreted by tumor cells and the surrounding stroma stimulates the proliferation and survival of endothelial cells, leading to the formation of new blood vessels, which may be structurally abnormal and leaky. Studies of VEGF biology have provided tremendous insights into physiological homeostasis and the molecular mechanisms of cancers. These discoveries have also illuminated our understanding of the complex interactions between VEGF and other signaling pathways [29].

In the present study, we aimed to explore the effects of ovarian cancer-derived extracellular vesicles (OV-EVs) on macrophage polarization and cancer progression. In addition, we conducted additional experiments to elucidate the mechanisms of EV-mediated angiogenesis in remodeling the TME.

Methods and materials

Study approval

All animal procedures were performed in accordance with the protocol approved by the Institutional Animal Care and Use Committee at Fudan University (SYXK2020-0032). This study was approved by the Obstetrics and Gynecology Hospital of Fudan University Institutional Review Board, approval number 2019–77, with informed consent obtained from all patients.

Cells and cell culture

The ovarian cancer cell lines SKOV3, ID-8, THP-1 and HUVECs (human umbilical vein endothelial cells) were purchased from the Chinese Academy of Sciences. We cultured SKOV3, ID-8, and THP-1 cells and HUVECs in DMEM supplemented with 10% fetal bovine serum and 1% penicillin/streptomycin. All the cells were cultured at 37 °C with 5% CO2 and 95% air, which were free of contamination.

Isolation of extracellular vesicles

SKOV3 cells were cultured to 70% confluence and then cultured with medium (containing extracellular vesicle-free FBS) for 48 h. The supernatant of the SKOV3 cells was collected for further EV isolation. We centrifuged the collected supernatant at 300 × g for 20 min and then at 10,000 × g for 60 min. Then, we conducted ultracentrifugation at 120,000 × g for 2 h at 4 °C to isolate the EVs. The EV pellet was washed with PBS to purify the isolated extracellular vesicles.

Characterization of extracellular vesicles

We characterized the shape of the collected extracellular vesicles via transmission electron microscopy (TEM) (FEI Tecnai G2 Spirit Twin, Philips, NL). We also characterized the diameters and the population of collected extracellular vesicles using a NanoSight NS300 (Malvern, Amesbury, GB). In addition, we tested the expression of extracellular vesicle markers in the collected extracellular vesicles through Western blotting.

Clinical samples

Fresh peripheral blood and fresh tumor tissues were collected from patients who were diagnosed with OV ($n = 10$) and non-OV ($n = 10$) donors at the Obstetrics and Gynecology Hospital of Fudan University from

January 2018 to December 2020. Peripheral blood mononuclear cells (PBMCs) were isolated by Ficoll density centrifugation using Ficoll-PaqueTM (GE Healthcare, NJ). Monocytes were isolated from PBMCs using a MACS isolation kit (Miltenyi Biotec, Aubum, CA) with positive selection for CD14 (Miltenyi Biotec). Fresh tissues were detached with collagenase IV and subsequently passed through a 70 μm cell strainer (Corning).

Cell viability assay

The viability of the cells was detected via CCK-8 assays. First, we seeded 5×10^3 HUVECs (human umbilical vein endothelial cells) per well into a 96-well plate and incubated them for 12 h. Then, we treated HUVECs with blank medium, conditioned medium from SKOV3 cells, or PBS (as a control). After incubation for 48 h, 10 μl/well CCK-8 (Dojindo, Japan) reagent was used to evaluate cell viability, which was measured by the OD450 value using a Varioskan LUX microplate reader (Thermo Fisher Scientific).

Tube formation assay

Angiogenic capacity was analyzed by a tube formation assay. First, we prepared a 24-well plate (30 μl of Matrigel (#356,234, BD Biosciences, Oxford, UK) per well). For this assay, a transwell coculture system was used to culture HUVECs with PBS, blank medium-induced macrophages or OV-EV-induced macrophages for 24 h. Then, we collected the HUVECs and seeded them (10^5 cells per well in a 24-well plate) into the prepared well (covered with Matrigel), after which they were cultured for 3 h. Tube formation was captured via microscopy (Leica DMi1), images of tube morphology were obtained at × 100 magnification, and the number of meshes was quantified via ImageJ software (NIH Image, Bethesda, MD).

Inducing polarization assay

We cultured THP-1 cells induced with phorbol 12-myristate-13-acetate (PMA) (100 ng/ml) for 24 h to induce the M0 phenotype. We treated M0 macrophages with culture supernatant or extracellular vesicles. Then, we detected the proportion of CD163 + cells via flow cytometry to quantify the percentage of macrophage polarization. All the experiments were repeated three times.

Immunofluorescence assay

The HUVECs were seeded on autoclaved slides, which were placed in a 24-well plate. The cells were then treated for 72 h with either the supernatant from OV-EV-treated macrophages, the supernatant from blank medium-treated macrophages or PBS. Then, we fixed the cells with 4% paraformaldehyde, followed by incubation with a FITC-VEGFR antibody for 30 min. Images were captured by confocal laser scanning microscopy (Leica Microsystems, Wetzlar, GER) at different laser channels. The images were merged, and all the images were evaluated and quantified via ImageJ software (NIH Image, Bethesda, MD).

Uptake process of EVs

The THP-1 cells were seeded on autoclaved slides, which were placed in a 24-well plate. Then, the isolated OV-EVs were stained with PKH-26 (Cell Linker Kit for General Membrane Labeling) for 30 min and reisolated via ultracentrifugation. The PKH-26-labeled EVs were added to the wells for 24 h. The cells were fixed with 4% paraformaldehyde and stained with FITC-Actin Tracker, followed by staining with DAPI for 10 min. Images were captured by confocal laser scanning microscopy (Leica Microsystems, Wetzlar, GER) at different laser channels. The images were merged, and all the images were evaluated and quantified via ImageJ software (NIH Image, Bethesda, MD).

Western blot

Extracellular vesicles were lysed in RIPA buffer. The protein concentration was determined via the BCA method. A total of 20 μg of protein was loaded on a 10%-12% SDS–PAGE gel. The proteins were transferred to a PVDF membrane and blocked in 5% BSA for 12 h at 4 °C. After being washed with 1 × TBST, the membrane was incubated with the following antibodies: CD63 (ab134045, 1:1,000), Tsg101 (ab13e586, 1:1,000) and Syntenin (ab133267, 1:1,000) overnight at 4 °C. After being washed with 1 × TBST three times, the membrane was incubated with HRP-conjugated secondary antibodies. The membranes were visualized with enhanced chemiluminescence.

Immunohistochemistry

The mouse tumor tissue sections were assessed by two experienced pathologists without discrepancy in our hospital. The working dilution of anti-VEGFR antibodies (ab11939; Abcam) was 1:100. The slides were washed and incubated with a biotinylated secondary antibody (polyclonal goat anti-rabbit; Histostain-Plus IHC kit; Mingrui Biotech, Shanghai, China) for 45 min at 37 °C and washed with PBS. To ensure uniformity, all the tissue sections were processed simultaneously.

ELISA

An ELISA was conducted to analyze the expression level of VEGF. We treated the cells with different types of media and collected the cell supernatants for ELISA. The

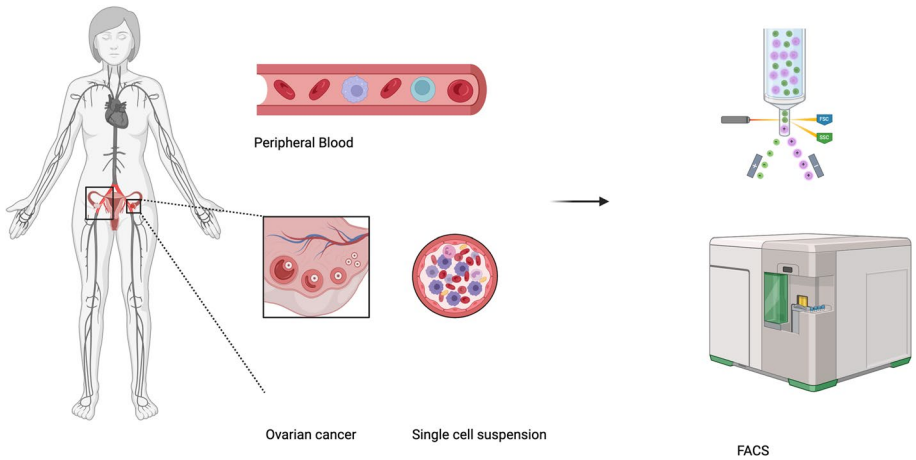

Fig. 1 Flowchart of the evaluation of macrophage subpopulations in ovarian tissues and peripheral blood from patients. Ovarian cancer tissues, nonovarian cancer tissues, and peripheral blood were obtained and then analyzed via flow cytometry to evaluate the macrophage subpopulations

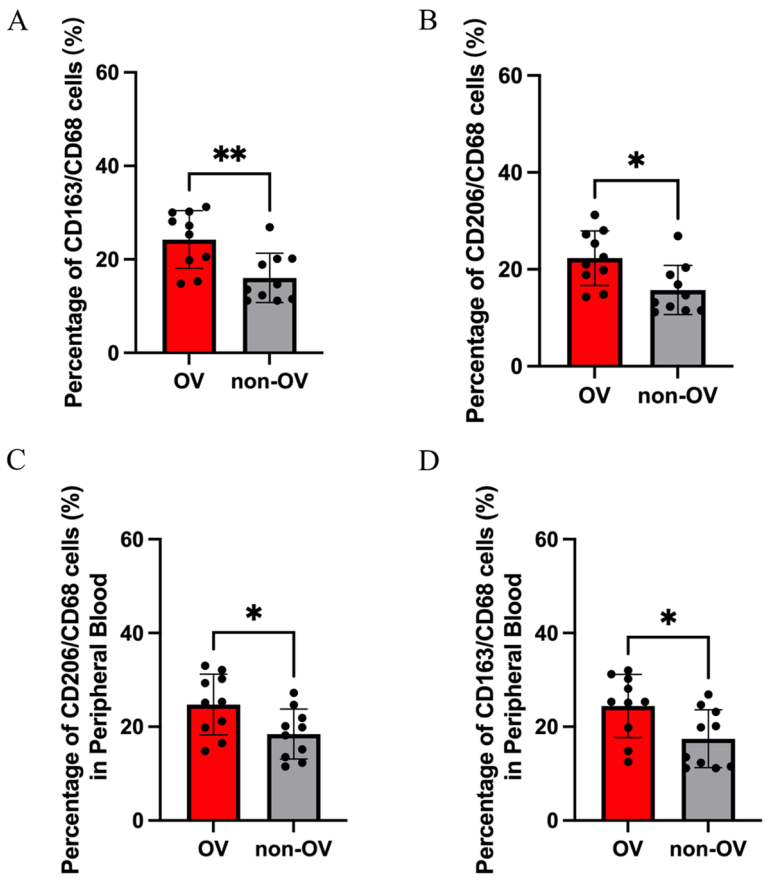

Fig. 2 Relationships of M2 phenotype expression in ovarian cancer tissues and peripheral blood. **A** The percentage of CD163 + CD68 + cells among CD68 + macrophages in ovarian cancer tissues and nonovarian cancer tissues from patients. **B** The percentage of CD206 + CD68 + cells among CD68 + macrophages in ovarian cancer tissues and nonovarian cancer tissues from patients. **C** The percentage of CD206 + CD68 + cells among CD68 + macrophages in the peripheral blood of patients. **D** The percentage of CD206 + CD68 + cells among CD68 + macrophages in the peripheral blood of patients

detection of the serum levels of VEGF was conducted via ELISA kits (Yanhui, Shanghai, China). (***$p < 0.001$).

Flow cytometry

Single-cell suspensions were blocked with mouse FcR blocking reagent (Miltenyi Biotec) for 10 min at 4 °C prior to surface staining. The following anti-mouse antibodies were used: FITC-conjugated CD11b, APC-conjugated CD163, and APC-conjugated CD206 from Biolegend. All flow cytometry data were acquired on a FACS Calibur (BD, San Jose, USA) and analyzed with FlowJo V10.8 (TreeStar, Ashland, USA).

Animal experiments

The animal experiments were conducted in accordance with the criteria for the Care and Use of Laboratory Animals and approved by the Ethics Committee of Obstetrics and Gynecologic Hospital of Fudan University (Ethics No. SYXK2020-0032). For the in vivo experiment, six-week-old female athymic nude mice (purchased from Jiesijie Laboratory Animal Co., Ltd., Shanghai) were divided randomly into three different subgroups as described below (three mice per group). Group #1 was the OV-EV group, group #2 was the M0-EV group, and group #3 was the PBS group. Briefly, as depicted in Fig. 7, SKOV3-luciferase stably transfected cells (treated with GW4869 (10 μM), an extracellular vesicle inhibitor) were seeded via intraperitoneal injection at a concentration of 1.5×10^6/mL per mouse on Day 0. Then, the ovarian cancer-derived extracellular vesicles (OV-EVs) (E^{11} particles/mouse per time), M0-derived extracellular vesicles (M0-EVs) (E^{11}/mouse per time), and PBS were intraperitoneally injected into groups #1, #2, and #3 on Days 3, 6, 9, 12, 15, and 18 (Fig. 7). Moreover, the mice were treated with GW4869 (200 μL/mouse, 0.3 mg/mL) every two days to inhibit the secretion of EVs by the tumor cells. We analyzed the ability of stably transfected SKOV3-luciferase cells to metastasize using an in vivo bioluminescence imaging system. The mice were sacrificed, and then the tumors were harvested. Half of the tumor tissues were fixed with PFA, and the other half were dissociated into a single-cell suspension. The slides with tumor tissue were stained to detect CD31, VEGFR and CD206 expression, and the single-cell suspensions were subjected to flow cytometry to measure the percentage of CD206-positive cells in the whole tumor tissues. Peripheral blood

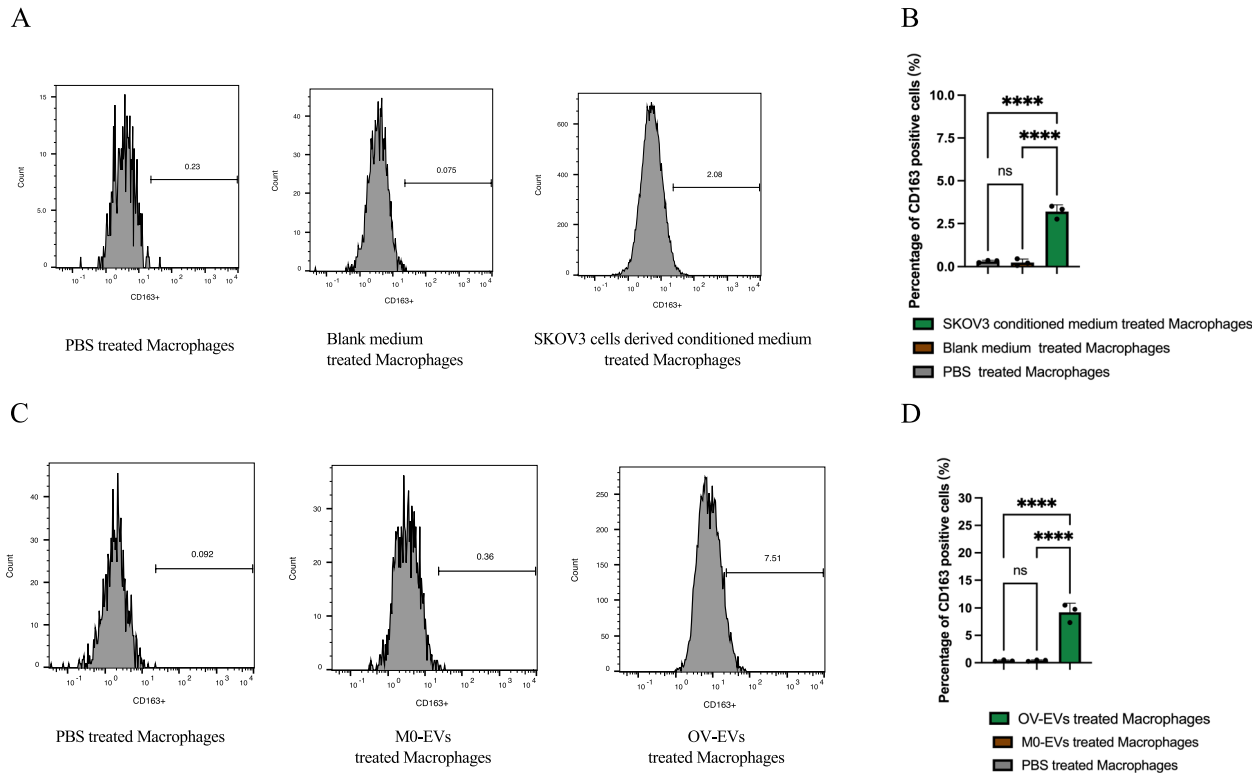

Fig. 3 Effects of ovarian cancer on the polarization of macrophages. **A** The expression levels of CD163 (M2 macrophage marker) in THP-1 cells after treatment with PBS (left), blank medium (middle), or ovarian cancer-conditioned medium (right). **B** Quantitative image of CD163 expression in macrophages. **C** The expression levels of CD163 (M2 macrophage marker) in THP-1 cells after treatment with PBS (left), M0-EVs (middle), or OV-EVs (right). **D** Quantitative image of CD163 expression in macrophages. The figure shows data from one out of three independent experiments performed in triplicate with equivalent results

mononuclear cells (PBMCs) were isolated by Ficoll density centrifugation using Ficoll-PaqueTM (GE Healthcare, NJ). Monocytes were isolated from PBMCs using a MACS isolation kit (Miltenyi Biotec, Aubum, CA) with positive selection for CD14 (Miltenyi Biotec).

Statistical analysis

All the experiments were repeated in triplicate, and the experimental results are expressed as the means ± standard deviations (S.D.). The statistical analysis was conducted via SPSS 19.0 software and GraphPad Prism 9.3 software.

Results

Relationships between the M2 phenotype and ovarian cancer

As shown in the flowchart in Fig. 1, flow cytometry was conducted on ovarian tissue and peripheral blood derived from patients with ovarian cancer and nonovarian cancer to evaluate the macrophage distribution. As shown in Fig. 2A and B, we observed increased expression of CD163 and CD206 (classic markers of M2 macrophages) in whole CD68 + macrophages (CD68 as a classic marker of macrophages) in ovarian tissues (Supplementary Figure S1, S1A and S1B). Similarly, as shown in Fig. 2C and D, we also observed increased expression of CD163 + and CD206 + CD68 + macrophages in the peripheral blood of ovarian cancer patients (Supplementary Figure S1, S1C and S1D).

Effects of ovarian cancer cells on the induction of macrophage polarization

To explore the effect of ovarian cancer on macrophage polarization, we evaluated the proportion of CD163 + (M2 macrophage marker) cells through flow cytometry. As depicted in Fig. 3A and B, macrophages expressed high levels of CD163 when they were treated with ovarian cancer cell-derived conditioned medium. These results indicate that ovarian cancer cell-derived conditioned medium could play a role in inducing macrophage polarization toward the M2 phenotype. As shown in Fig. 3C and D, macrophages expressed high levels of CD163 when they were treated with ovarian cancer cell-derived extracellular vesicles (OV-EVs). These results indicate that ovarian cancer cell-derived EVs could play a role in inducing macrophage polarization toward the M2 phenotype.

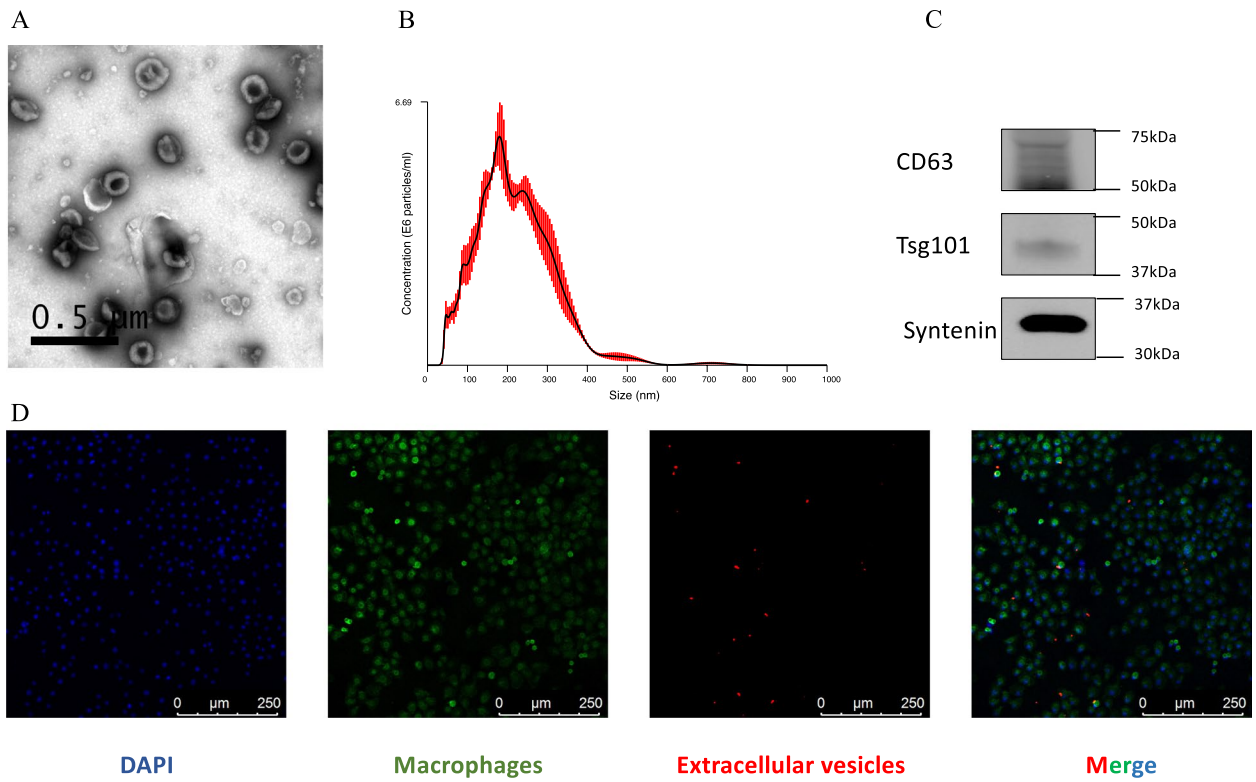

Fig. 4 Characterization of extracellular vesicles. **A** Transmission electron microscopy characterization of extracellular vesicles derived from SKOV3 ovarian cancer cells. Scale bars, 0.5 μm. **B** NTA characterization of extracellular vesicles derived from SKOV3 ovarian cancer cells. **C** Western blot characterization of extracellular vesicles: the expression of CD63, Tsg101 and syntenin in extracellular vesicles derived from SKOV3 ovarian cancer cells. **D** Evaluation of PKH-26-labeled EVs encapsulated by FITC-labeled THP-1 cells. Scale bars, 250 μm

Isolation and characterization of extracellular vesicles

We isolated extracellular vesicles from ovarian cancer cell-conditioned medium via ultracentrifugation. We characterized the extracellular vesicles through diverse methods, including TEM, NTA and Western blotting. The shape of the OV-EVs was measured by transmission electron microscopy (Fig. 4A). Moreover, the size distribution and characterization of the OV-EVs were analyzed by nanoparticle tracking analysis (NTA) (Fig. 4B). Furthermore, markers of OV-EVs were detected via Western blotting (Fig. 4C, Supplementary Figure S2). Thus, these results indicate that the particles collected from the conditioned medium are extracellular vesicles. In addition, PKH-26-labeled OV-EVs were encapsulated in FITC-actin tracker-labeled THP-1 cells (Fig. 4D). The lipid bilayers of OV-EVs were stained with PKH-26 (Cell Linker Kit for General Membrane Labeling), while those of THP-1 cells were labeled with FITC-Actin Tracker. Overall, these data indicate that the isolated OV-EVs (with a normal size and shape) were able to enter the recipient cells (THP-1 cells).

Effects of ovarian cancer extracellular vesicle (OV-EV)-treated macrophages on angiogenesis

To evaluate the influence of ovarian cancer-derived extracellular vesicle (OV-EV)-treated macrophages on angiogenic capacity and proliferative capacity, we conducted a cell viability assay and a tube formation assay with HUVECs. As clearly shown in Fig. 5A and B, compared with M0-EV-induced macrophages and PBS, OV-EV-induced macrophages exhibited increased tube formation ability. However, OV-EV-induced macrophages did not significantly promote HUVEC proliferation when compared with the M0-EV-induced macrophage group

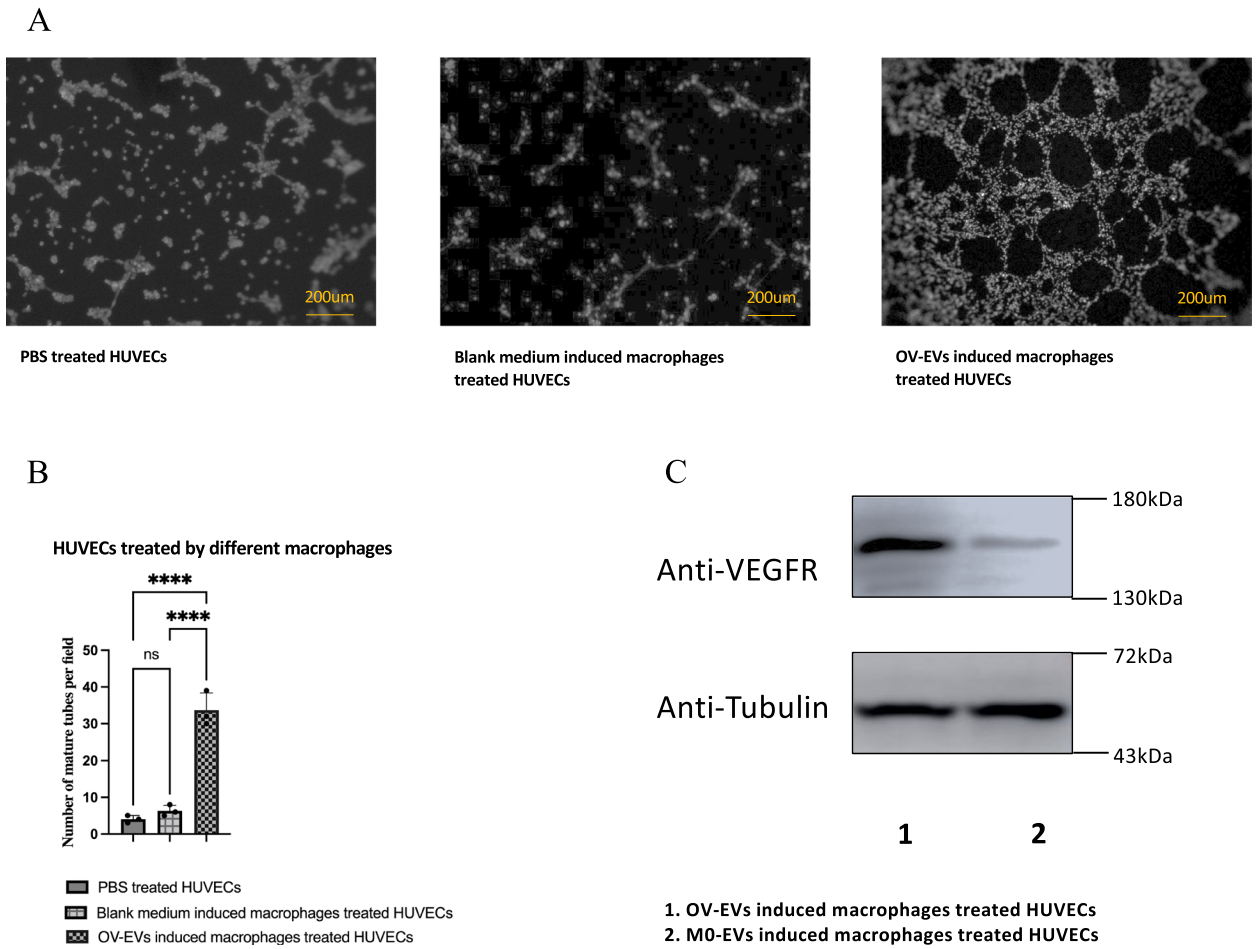

Fig. 5 Influence of ovarian cancer-derived extracellular vesicles on angiogenic capacity. **A** Representative images of the tube formation ability of HUVECs treated with PBS (Left), HUVECs treated with M0-EVs induced macrophages (Middle), and HUVECs treated with OV-EVs treated with macrophages (Right). **B** Quantitative image of the formation ability of HUVECs. The figure shows data from one out of three independent experiments performed in triplicate with equivalent results. **C** The expression level of VEGF in OV-EV-treated macrophages and M0-EV-induced macrophages

or PBS group (Supplementary Figure S3, S3A). Moreover, OV-EVs did not promote HUVEC proliferation (Supplementary Figure S3, S3B). These results indicate that ovarian cancer-derived extracellular vesicles (OV-EVs) promote macrophage-mediated angiogenesis during cancer progression. Furthermore, as depicted in Fig. 5C (Supplementary Figure S4), OV-EV-treated macrophages induced the expression of VEGFR on HUVECs.

OV-EVs promote the secretion of VEGF by macrophages to induce angiogenesis

To explore the mechanism of the increased angiogenic capacity induced by OV-EV-treated macrophages, we detected VEGFR expression on HUVECs following different EV treatments. We first detected VEGF expression in OV-EV-treated macrophages, M0-EV-treated macrophages and PBS-treated macrophages via ELISA. As depicted in Fig. 6, the results revealed that VEGF expression was significantly greater in the group treated with OV-EV-induced macrophages than in the M0-EV-treated macrophage group or the PBS-treated macrophage group (Fig. 6A). Moreover, as depicted in Fig. 6B, OV-EV-induced macrophages stimulated the expression of VEGFR (VEGF receptor) in HUVECs, whereas blank medium-treated macrophages and PBS-treated macrophages did not induce VEGFR expression in HUVECs. As depicted in Fig. 6C and D, OV-EV-induced macrophages stimulated the expression of VEGFR (VEGF receptor) in HUVECs, whereas M0-EV-treated macrophages and PBS-treated macrophages did not induce

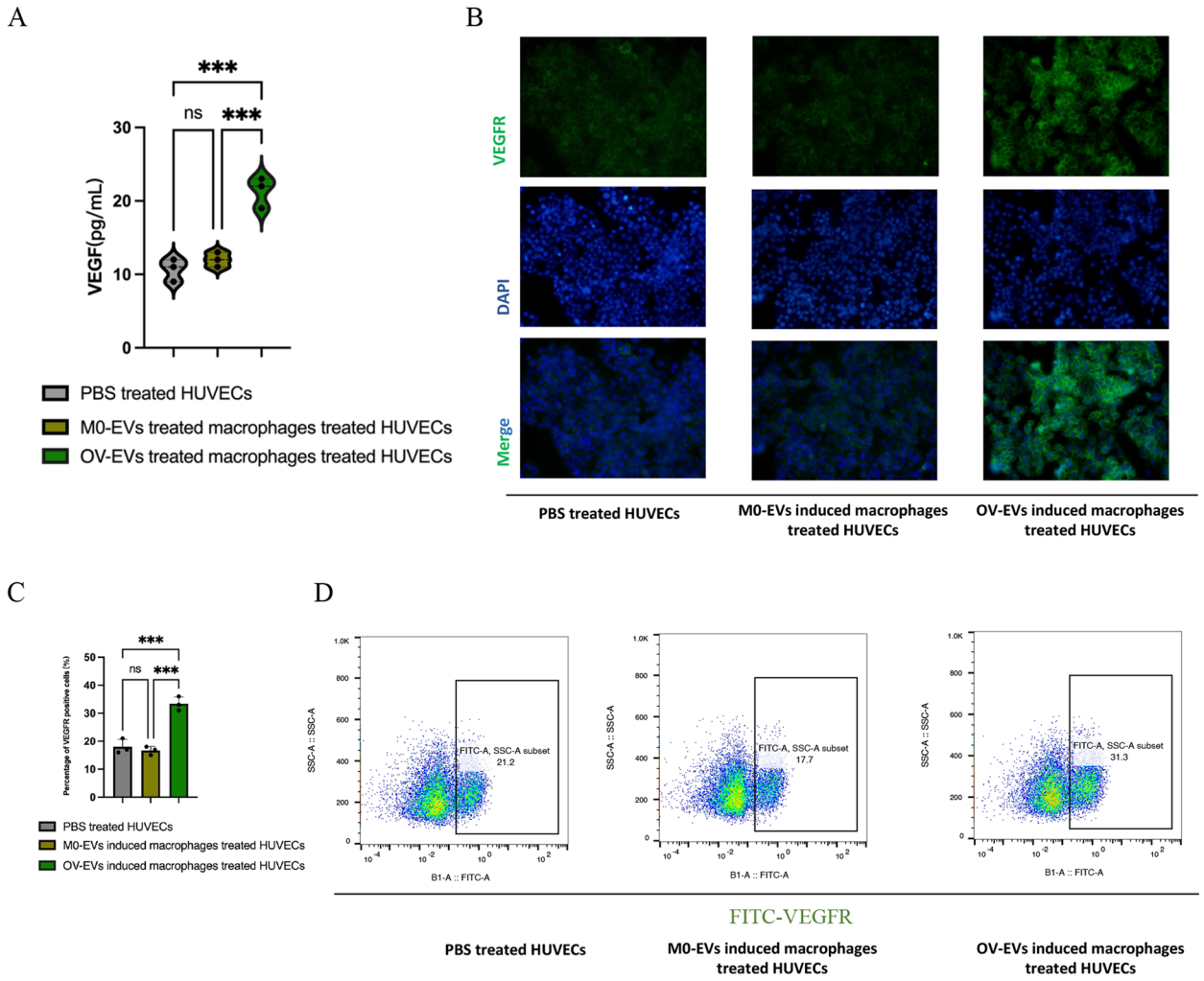

Fig. 6 The expression levels of VEGF in macrophages and VEGFR in HUVECs after treatment with OV-EVs. **A** The expression level of VEGF in OV-EV-induced macrophages, M0-EV-induced macrophages and PBS-treated macrophages. **B** The expression of DAPI and VEGFR on the cell surface of HUVECs after treatment with OV-EV-induced macrophages, M0-EV-induced macrophages, or PBS. **C** Quantitative image of VEGFR expression in HUVECs. **D** VEGFR expression level in HUVECs after treatment with OV-EV-induced macrophages, M0-EV-induced macrophages and PBS. The figure shows data from one out of three independent experiments performed in triplicate with equivalent results

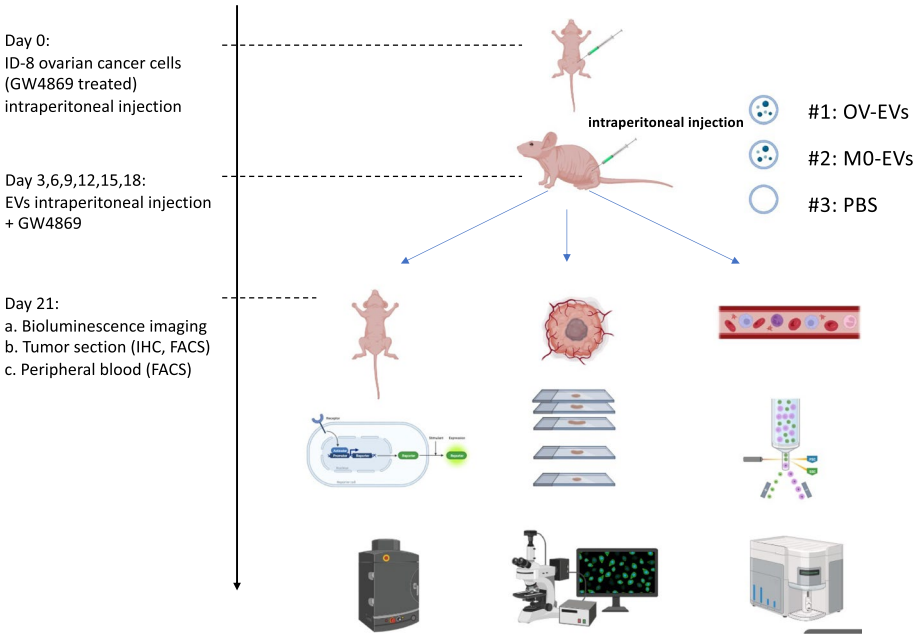

Fig. 7 Flow chart of the animal experiment. The mice were grouped, and the cancer cells were seeded on Day 0 and treated on Days 3, 6, 9, 12, 15, and 18, followed by sacrifice on Day 21. For the animal assay, SKOV3-luciferase stable cells (treated with GW4869) were seeded in nude mice. The mice in the OV-EV group were treated with OV-EVs, those in the M0-EV group were treated with M0-EVs, and those in the PBS group were treated with PBS. The expression of bioluciferase and specific expression levels in tumor slides and in single cells derived from tumor tissues as well as peripheral blood were detected via a bioluminescence imaging system, IHC and flow cytometry

VEGFR expression in HUVECs. Taken together, these results indicate that OV-EV-induced macrophages play a role in inducing angiogenesis.

OV-EVs promote ovarian cancer progression by promoting the expression of VEGFR in vascular endothelial cell-induced M2 macrophages in vivo

As depicted in Fig. 7, we conducted an animal experiment using SKOV3-luciferase stably transfected cells (treated with GW4869) to analyze the influence of OV-EV-induced macrophages on the progression of ovarian cancer. We divided the animals into three groups ($n=3$ mice per group): the OV-EV group, the M0-EVs group, and the PBS group. We detected the cancer progression of ovarian cancer cells by measuring the luminescence of SKOV3-luciferase cells using an in vivo imaging system (Fig. 7). As shown in Fig. 8A and B, OV-EVs promoted the progression of ovarian cancer. As shown in Fig. 8C and D, OV-EVs induced the expression of VEGFR in excised tumor tissues, as determined by immunohistochemistry, and the expression level of VEGFR in the OV-EV group was greater than that in the other two groups. The induced M2 macrophages promoted VEGFR expression in tumor tissues, which mediated angiogenesis during cancer progression. As depicted in Fig. 8E and F, OV-EVs increased CD31 expression in tumors. In addition, OV-EVs induced increased CD206 expression in tumors (Fig. 8G and H). Furthermore, as depicted in Fig. 9A and B, OV-EVs increased F4/80 + CD163 + macrophage infiltration. Additionally, as depicted in Fig. 9C and D, OV-EVs increased F4/80 + CD206 + macrophage infiltration into tumors. As shown in Fig. 9E and F, OV-EVs induced

(See figure on next page.)

Fig. 8 The influence of ovarian cancer-derived EVs induced by macrophages on cancer progression and angiogenesis in vivo. **A** Representative images of the bioluminescence results were obtained to evaluate the metastasis of ovarian cancer after treatment with OV-EV-induced macrophages, M0-EV-induced macrophages, or PBS in a mouse model. **B** Representative images of IHC staining for detecting VEGFR expression in tumors ($n=3$). **C** Representative images of IHC (anti-VEGFR) images of tumors from model mice treated with OV-EVs, M0-EVs or PBS. Scale bars, 200 nm. **D** Quantitative image of VEGFR expression in tumor slides ($n=3$). **E** Representative images of IHC (anti-CD31) images of tumors from model mice treated with OV-EVs, M0-EVs or PBS. **F** Quantitative image of CD31 expression in tumor slides ($n=3$). **G** Representative images of IHC (anti-CD206) images of tumors from model mice treated with OV-EVs, M0-EVs or PBS. **H** Quantitative image of CD206 expression in tumor slides ($n=3$)

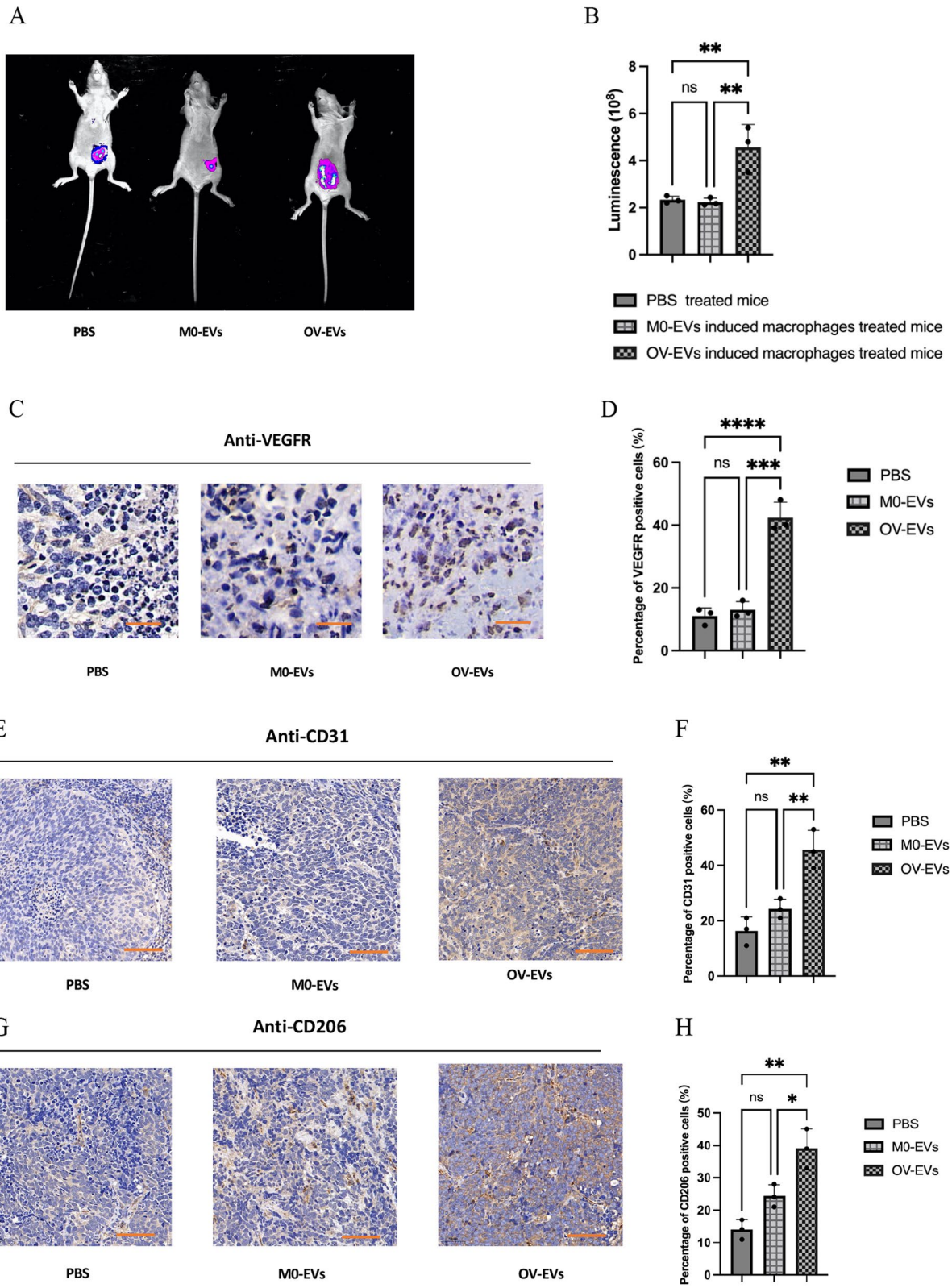

Fig. 8 (See legend on previous page.)

F4/80 + CD163 + macrophages in the whole peripheral blood. Additionally, as shown in Fig. 9G and H, OV-EVs induced more F4/80 + CD206 + macrophages in the whole peripheral blood (Fig. 9). Collectively, these results indicate that ovarian cancer-derived extracellular vesicles (OV-EVs) can induce macrophages to adopt the M2 phenotype and that M2 macrophages can infiltrate tumor tissues and promote VEGFR expression to aggravate cancer progression.

Discussion

Ovarian cancer is an intractable malignancy of the female reproductive system [30, 31]. Recently, increasing evidence has revealed the vital role of microenvironment regulation in ovarian cancer progression [32, 33]. However, clarifying the underlying mechanisms involved in the progression of ovarian cancer is still highly challenging. Macrophages reportedly participate in tumor progression through diverse types of communication and crosstalk with other cells in the tumor microenvironment [9, 34] and have been identified as potential therapeutic targets [7]. In the tumor microenvironment, macrophages can secrete diverse cytokines, which contribute to maintaining the inflammatory environment and promote cancer cell growth as well as cancer cell migration. Additionally, many studies have reported that tumor-associated macrophages (TAMs) are associated with aspects of cancer progression, including cancer proliferation [35], cancer metastasis [36], and cancer drug resistance [37]. Extracellular vesicles (EVs) are known as membrane-bound vesicles containing different molecules that are involved in the crosstalk among diverse cell types. Increasing amounts of clinical data and experimental evidence have shown that cancer cell-derived extracellular vesicles play vital roles in cancer progression, which provides new insights for improving current cancer therapeutic strategies.

To explore the detailed mechanisms underlying progression and angiogenesis, we first detected a subpopulation of M2 macrophages in ovarian cancer tissues and peripheral blood of patients. According to the results of flow cytometry analysis of ovarian cancer tissues and peripheral blood samples, both the percentages of CD163 + CD68 + cells and CD206 + CD68 + cells among total CD68 + macrophages in ovarian tissues and in peripheral blood samples were greater than those in nonovarian cancer samples. These findings indicate that the M2 subtypes of macrophages are enriched in ovarian cancer. These results are in line with those of previous studies [38, 39], which suggests that M2 macrophages play vital roles in cancer progression. Next, we detected the effect of ovarian cancer on macrophage polarization and found that ovarian cancer can induce macrophage polarization toward the M2 phenotype. Furthermore, to explore the role of M2 macrophages in ovarian cancer progression, we isolated extracellular vesicles from ovarian cancer cell-conditioned medium and characterized them via transmission electron microscopy, NTA and Western blotting, which are widely used methods. Remarkably, OC-EVs induced the macrophages toward the M2 phenotype. These results are in line with the results of previous studies from other groups [40, 41]. We then treated HUVECs with conditioned medium derived from induced M2 macrophages and found that M2 medium promoted the tube formation ability of HUVECs. In addition, OV-EVs induced macrophages to secrete VEGF, which may explain the mechanism of increased tube-formation capacity reported in previous studies [42, 43]. In animal experiments, we also found that ovarian cancer cell-derived extracellular vesicles induced M2 polarization in whole peripheral blood and M2 macrophage infiltration in tumors. These processes promoted the progression of ovarian cancer, which is in line with the in vitro results.

There are several limitations in the present study. First, more ovarian cancer tissue is needed for further analysis to verify the relationship between macrophage infiltration and ovarian cancer progression. Second, the ability of other types of cells in the tumor environment to perform similar functions during cancer progression should be explored.

Overall, the present study revealed the vital roles of OV-EVs in promoting macrophage polarization and subsequent angiogenesis. In addition, this study provides novel insights into the role of cancer-derived EVs in inducing macrophage polarization and regulating endothelial cells in the tumor microenvironment.

(See figure on next page.)

Fig. 9 The percentage of M2 macrophages in tumor tissues and in whole peripheral blood of treated mice. **A** The percentage of CD163-positive macrophages in single-cell suspensions of tumors. **B** Quantitative image of CD163-positive macrophages in a single-cell suspension of tumors. **C** The percentage of induced CD206-positive macrophages in single-cell suspensions of tumors. **D** Quantitative image of CD206-positive macrophages in a single-cell suspension of tumors. **E** The percentage of CD163-positive macrophages in the peripheral blood of the mice. **F** Quantitative image of CD163-positive macrophages in the peripheral blood of mice. **G** The percentage of CD206-positive macrophages in the peripheral blood of the mice. **H** Quantitative image of CD206-positive macrophages in the peripheral blood of mice. The figure shows data from one out of three independent experiments performed in triplicate with equivalent results

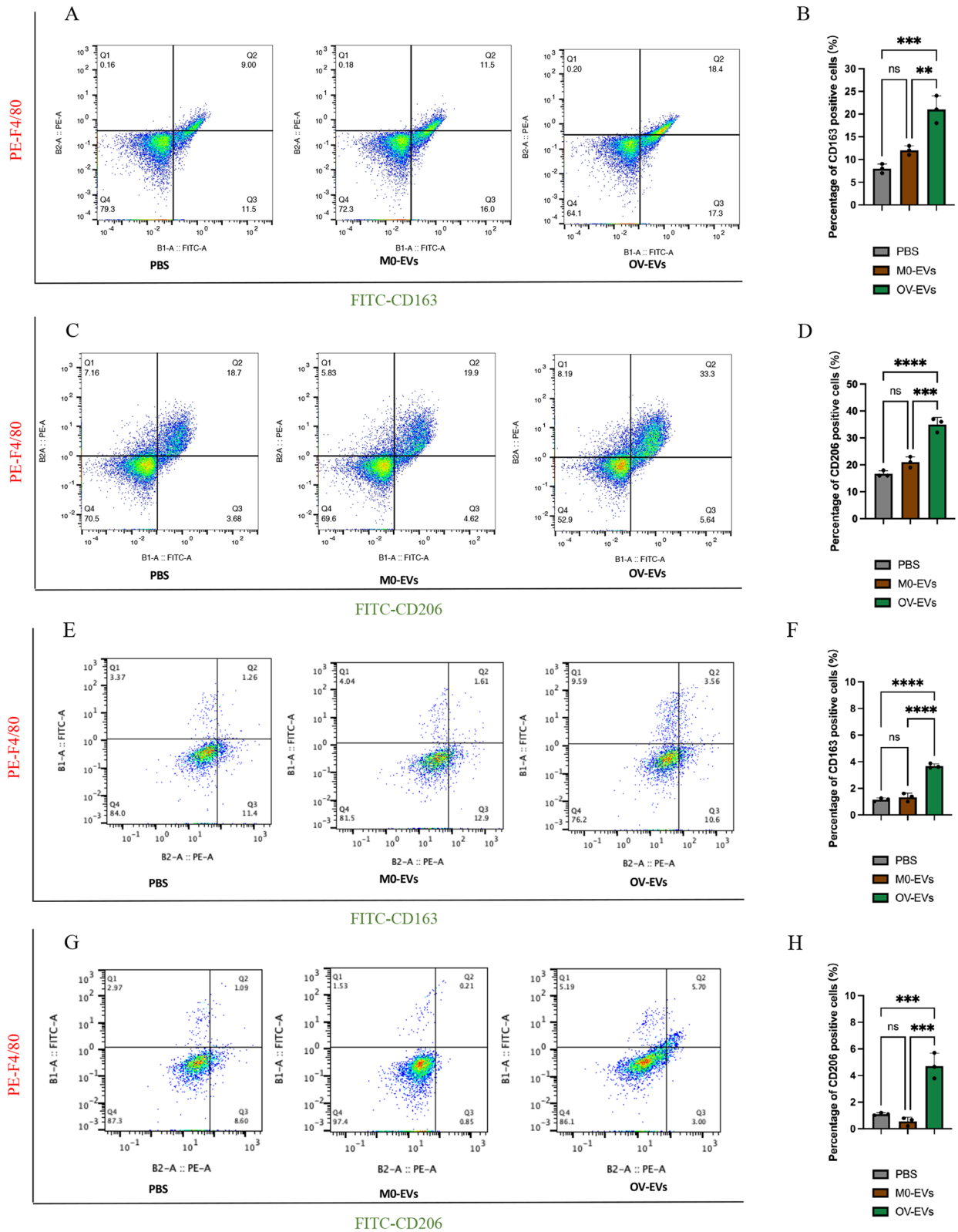

Fig. 9 (See legend on previous page.)

Conclusions

We demonstrated that ovarian cancer-derived extracellular vesicles (OV-EVs) can contribute to the progression of ovarian cancer through skewing M2 macrophage polarization. Additionally, OV-EV-induced M2 macrophages enhanced the angiogenic capacity of HUVECs. Furthermore, we revealed that OV-EV-induced macrophages can enhance angiogenesis by increasing the expression level of VEGF. Overall, our study has elucidated a novel molecular mechanism involving ovarian cancer, macrophages and vascular endothelial cells in the tumor microenvironment. While it is known that EVs can function as messengers between ovarian cancer cells and macrophages, these results provide new insights into the development (including the progression and remodeling of the microenvironment) of ovarian cancer as well as a theoretical basis for future treatment strategies for ovarian cancer. Moreover, extracellular vesicle-mediated crosstalk between tumor cells and macrophages may constitute a novel targeting strategy for ovarian cancer therapeutics.

Supplementary Information

The online version contains supplementary material available at https://doi.org/10.1186/s13048-024-01497-y.

Supplementary Material 1: Supplementary Figure S1. Representative images of flow cytometry used to detect the M2 phenotype subpopulation in ovarian cancer tissues and peripheral blood. A. Representative images of the percentage of CD163 + CD68 + cells among CD68 + macrophages in ovarian cancer tissues and nonovarian cancer tissues from patients. B. Representative images of the percentage of CD206 + CD68 + cells among CD68 + macrophages in ovarian cancer tissues and nonovarian cancer tissues from patients. C. Representative images of the percentage of CD206 + CD68 + cells among CD68 + macrophages in the peripheral blood of patients. D. Representative images of the percentage of CD206 + CD68 + cells among CD68 + macrophages in the peripheral blood of patients.

Supplementary Material 2: Supplementary Figure S2. Western blot image of extracellular vesicles: the expression of CD63, Tsg101 and syntenin in extracellular vesicles derived from SKOV3 ovarian cancer cells.

Supplementary Material 3: Supplementary Figure S3. A. Proliferation of HUVECs treated with different macrophages. B. Proliferation of HUVECs treated with different EVs. The figure shows data from one out of three independent experiments performed in triplicate with equivalent results.

Supplementary Material 4: Supplementary Figure S4. Western blot image of VEGFR expression in HUVECs. VEGFR expression in OV-EVs induced macrophage-treated HUVECs, and M0-EVs induced macrophage-derived HUVECs.

Supplementary Material 5.

Supplementary Material 6.

Authors' contributions

X.T. and CB.M. wrote the main manuscript text, and QW.W. prepared figures. M.Y. polished and reviewed the manuscript. All authors reviewed the manuscript.

Funding

The study was funded by the Scientific Research Project of Changning District Science and Technology Commission (CNKW2022Y32).

Availability of data and materials

In this manuscript, data that support the findings of this study are available on request from the corresponding author. Inquiries should be communicated with the corresponding author, and we will consider all sufficiently specified and reasonable requests.

Data availability

No datasets were generated or analysed during the current study.

Declarations

Ethics approval and consent to participate

All animal procedures were performed in accordance with the protocol approved by the Institutional Animal Care and Use Committee at Fudan University (SYXK2020-0032).

Competing interests

The authors declare no competing interests.

Received: 5 February 2024 Accepted: 14 August 2024
Published online: 24 August 2024

References

1. Armstrong DK, Alvarez RD, Bakkum-Gamez JN, et al. Ovarian Cancer, Version 2.2020, NCCN Clinical Practice Guidelines in Oncology. J Natl Compr Canc Netw. 2021;19(2):191–226. https://doi.org/10.6004/jnccn.2021.0007.
2. Christian J, Thomas H. Ovarian cancer chemotherapy. Cancer Treat Rev. 2001;27(2):99–109. https://doi.org/10.1053/ctrv.2001.0219.
3. Lee W, Ko SY, Mohamed MS, Kenny HA, Lengyel E, Naora H. Neutrophils facilitate ovarian cancer premetastatic niche formation in the omentum. J Exp Med. 2019;216(1):176–94. https://doi.org/10.1084/jem.20181170.
4. Rosati A, De Rose AM, Sala E, Giuliante F, Scambia G, Fagotti A. Ovarian cancer metastases in the liver area: proposal of a standardized anatomo-surgical classification. Int J Gynecol Cancer. 2022;32(7):955–6. https://doi.org/10.1136/ijgc-2021-003307.
5. Lan J, Sun L, Xu F, et al. M2 Macrophage-Derived Exosomes Promote Cell Migration and Invasion in Colon Cancer. Cancer Res. 2019;79(1):146–58. https://doi.org/10.1158/0008-5472.CAN-18-0014.
6. DeNardo DA-O, Ruffell B. Macrophages as regulators of tumour immunity and immunotherapy. Nat Rev Immunol. 2019;19(6):369–82. https://doi.org/10.1038/s41577-019-0127-6.
7. Pathria P, Louis TL, Varner JA. Targeting Tumor-Associated Macrophages in Cancer. Trends Immunol. 2019;40(4):310–27. https://doi.org/10.1016/j.it.2019.02.003.
8. Shapouri-Moghaddam A, Mohammadian S, Vazini H, et al. Macrophage plasticity, polarization, and function in health and disease. J Cell Physiol. 2018;233(9):6425–40. https://doi.org/10.1002/jcp.26429.
9. Ma RY, Black A, Qian BZ. Macrophage diversity in cancer revisited in the era of single-cell omics. Trends Immunol. 2022;43(7):546–63. https://doi.org/10.1016/j.it.2022.04.008.
10. Funes SC, Rios M, Escobar-Vera J, Kalergis AM. Implications of macrophage polarization in autoimmunity. Immunology. 2018;154(2):186–95. https://doi.org/10.1111/imm.12910.
11. Kim SY, Nair MG. Macrophages in wound healing: activation and plasticity. Immunol Cell Biol. 2019;97(3):258–67. https://doi.org/10.1111/imcb.12236.
12. Dong F, Ruan S, Wang J, et al. M2 macrophage-induced lncRNA PCAT6 facilitates tumorigenesis and angiogenesis of triple-negative breast cancer through modulation of VEGFR2. Cell Death Dis. 2020;11(9):728. https://doi.org/10.1038/s41419-020-02926-8.
13. Lopez-Yrigoyen M, Cassetta L, Pollard JW. Macrophage targeting in cancer. Ann N Y Acad Sci. 2021;1499(1):18–41. https://doi.org/10.1111/nyas.14377.
14. Li W, Zhang X, Wu F, et al. Gastric cancer-derived mesenchymal stromal cells trigger M2 macrophage polarization that promotes metastasis and EMT in gastric cancer. Cell Death Dis. 2019;10(12):918. https://doi.org/10.1038/s41419-019-2131-y.

15. Epstein RJ. VEGF signaling inhibitors: more pro-apoptotic than anti-angiogenic. Cancer Metastasis Rev. 2007;26(3–4):443–52. https://doi.org/10.1007/s10555-007-9071-1.
16. Zhang J, Muri J, Fitzgerald G, et al. Endothelial Lactate Controls Muscle Regeneration from Ischemia by Inducing M2-like Macrophage Polarization. Cell Metab. 2020;31(6):1136-1153.e7. https://doi.org/10.1016/j.cmet.2020.05.004.
17. Théry CA-O, Witwer KA-O, Aikawa E, et al. Minimal information for studies of extracellular vesicles 2018 (MISEV2018): a position statement of the International Society for Extracellular Vesicles and update of the MISEV2014 guidelines. J Extracell Vesicles. 2018;7(1):1535750. https://doi.org/10.1080/20013078.2018.1535750.
18. Hoshino A, Kim HS, Bojmar L, et al. Extracellular Vesicle and Particle Biomarkers Define Multiple Human Cancers. Cell. 2020;182(4):1044–61.e18. https://doi.org/10.1016/j.cell.2020.07.009.
19. Zhou G, Gu Y, Zhu Z, et al. Exosome Mediated Cytosolic Cisplatin Delivery Through Clathrin-Independent Endocytosis and Enhanced Anti-cancer Effect via Avoiding Endosome Trapping in Cisplatin-Resistant Ovarian Cancer. Front Med (Lausanne). 2022;3(9): 810761. https://doi.org/10.3389/fmed.2022.810761.
20. van Niel G, D'Angelo G, Raposo G. Shedding light on the cell biology of extracellular vesicles. Nat Rev Mol Cell Biol. 2018;19(4):213–28. https://doi.org/10.1038/nrm.2017.125.
21. Zhou G, Gu Y, Zhou F, et al. The Emerging Roles and Therapeutic Potential of Extracellular Vesicles in Infertility. Front Endocrinol (Lausanne). 2021;22(12): 758206. https://doi.org/10.3389/fendo.2021.758206.
22. Zhao H, Shang Q, Pan Z, et al. Exosomes From Adipose-Derived Stem Cells Attenuate Adipose Inflammation and Obesity Through Polarizing M2 Macrophages and Beiging in White Adipose Tissue. Diabetes. 2018;67(2):235–47. https://doi.org/10.2337/db17-0356.
23. Li Y, Tang X, Gu Y, Zhou G. Adipocyte-Derived Extracellular Vesicles: Small Vesicles with Big Impact. Front Biosci (Landmark Ed). 2023;28(7):149. https://doi.org/10.31083/j.fbl2807149.
24. Zhou G, Gu Y, Zhou F, et al. Adipocytes-Derived Extracellular Vesicle-miR-26b Promotes Apoptosis of Cumulus Cells and Induces Polycystic Ovary Syndrome. Front Endocrinol (Lausanne). 2021;12: 789939. https://doi.org/10.3389/fendo.2021.789939.
25. Zhou G, Gu Y, Zhou F, et al. The Emerging Roles and Therapeutic Potential of Extracellular Vesicles in Infertility. Front Endocrinol (Lausanne). 2021;12: 758206. https://doi.org/10.3389/fendo.2021.758206.
26. Dorayappan KDP, Wallbillich JJ, Cohn DE, Selvendiran K. The biological significance and clinical applications of exosomes in ovarian cancer. Gynecol Oncol. 2016;142(1):199–205. https://doi.org/10.1016/j.ygyno.2016.03.036.
27. Clement E, Lazar I, Attané CAO, et al. Adipocyte extracellular vesicles carry enzymes and fatty acids that stimulate mitochondrial metabolism and remodeling in tumor cells. EMBO J. 2020;39(3):e102525. https://doi.org/10.15252/embj.2019102525.
28. Ferrara N, Adamis AP. Ten years of anti-vascular endothelial growth factor therapy. Nat Rev Drug Discov. 2016;15(6):385–403. https://doi.org/10.1038/nrd.2015.17.
29. Apte RS, Chen DS, Ferrara N. VEGF in Signaling and Disease: Beyond Discovery and Development. Cell. 2019;176(6):1248–64. https://doi.org/10.1016/j.cell.2019.01.021.
30. Vergote I, Gonzalez-Martin A, Lorusso D, et al. Clinical research in ovarian cancer: consensus recommendations from the Gynecologic Cancer InterGroup. Lancet Oncol. 2022;23(8):e374–84. https://doi.org/10.1016/S1470-2045(22)00139-5.
31. Wu L, Zhu J, Yin R, et al. Olaparib maintenance therapy in patients with newly diagnosed advanced ovarian cancer and a BRCA1 and/or BRCA2 mutation: SOLO1 China cohort. Gynecol Oncol. 2021;160(1):175–81. https://doi.org/10.1016/j.ygyno.2020.10.005.
32. Zheng X, Wang X, Cheng X, et al. Single-cell analyses implicate ascites in remodeling the ecosystems of primary and metastatic tumors in ovarian cancer. Nat Cancer. 2023;4(8):1138–56. https://doi.org/10.1038/s43018-023-00599-8.
33. Wu X, Zhu JA-O, Wang J, et al. Pamiparib Monotherapy for Patients with Germline BRCA1/2-Mutated Ovarian Cancer Previously Treated with at Least Two Lines of Chemotherapy: A Multicenter, Open-Label. Phase II Study Clin Cancer Res. 2022;28(4):653–61. https://doi.org/10.1158/1078-0432.CCR-21-1186.
34. Hwang I, Kim JW, Ylaya K, et al. Tumor-associated macrophage, angiogenesis and lymphangiogenesis markers predict prognosis of non-small cell lung cancer patients. J Transl Med. 2020;18(1):443. https://doi.org/10.1186/s12967-020-02618-z.
35. Liu W, Wang W, Wang X, Xu C, Zhang N, Di W. Cisplatin-stimulated macrophages promote ovarian cancer migration via the CCL20-CCR6 axis. Cancer Lett. 2020;1(472):58–69. https://doi.org/10.1016/j.canlet.2019.12.024.
36. Qian BZ, Pollard JW. Macrophage diversity enhances tumor progression and metastasis. Cell. 2010;141(1):39–51. https://doi.org/10.1016/j.cell.2010.03.014.
37. Ruffell B, Coussens LM. Macrophages and therapeutic resistance in cancer. Cancer Cell. 2015;27(4):462–72. https://doi.org/10.1016/j.ccell.2015.02.015.
38. Jackute J, Zemaitis M, Pranys D, et al. Distribution of M1 and M2 macrophages in tumor islets and stroma in relation to prognosis of non-small cell lung cancer. BMC Immunol. 2018;19(1):3. https://doi.org/10.1186/s12865-018-0241-4.
39. Ran XM, Yang J, Wang ZY, Xiao LZ, Deng YP, Zhang KQ. M2 macrophage-derived exosomal circTMCO3 acts through miR-515–5p and ITGA8 to enhance malignancy in ovarian cancer. Commun Biol. 2024;7(1):583. https://doi.org/10.1038/s42003-024-06095-8.
40. Yang S, Zhao H, Xiao W, Shao L, Zhao C, Sun P. Extracellular vesicle-packaged miR-181c-5p from epithelial ovarian cancer cells promotes M2 polarization of tumor-associated macrophages via the KAT2B/HOXA10 axis. J Gene Med. 2022;24(10): e3446. https://doi.org/10.1002/jgm.3446.
41. Wang F, Niu Y, Chen K, et al. Extracellular Vesicle-Packaged circATP2B4 Mediates M2 Macrophage Polarization via miR-532-3p/SREBF1 Axis to Promote Epithelial Ovarian Cancer Metastasis. Cancer Immunol Res. 2023;11(2):199–216. https://doi.org/10.1158/2326-6066.Cir-22-0410.
42. Yin J, Forn-Cuní G, Surendran AM, et al. Lactate secreted by glycolytic conjunctival melanoma cells attracts and polarizes macrophages to drive angiogenesis in zebrafish xenografts. Angiogenesis. 2024. https://doi.org/10.1007/s10456-024-09930-y.
43. Westphal JR, Van't Hullenaar R, Peek R, et al. Angiogenic balance in human melanoma: expression of VEGF, bFGF, IL-8, PDGF and angiostatin in relation to vascular density of xenografts in vivo. Int J Cancer. 2000;86(6):768–76. https://doi.org/10.1002/(sici)1097-0215(20000615)86:6%3c768::aid-ijc3%3e3.0.co;2-e.

Publisher's Note